

Eli Lansey , Genevieve Hankins , Isroel Mandel , Richard Martelly ,
Jocelyn Slater , and Naomi R. Greenberg 

In Defense of Spheres for Computational Electromagnetics Code Validation and Benchmarking

Rethinking the sphere of influence.



©SHUTTERSTOCK.COM/PIXELPARTICLE

Digital Object Identifier 10.1109/MAP.2025.3537414
Date of current version: 3 April 2025

In this article, we illustrate some examples of how using spheres for computational electromagnetics (CEM) validation provides a range of challenges and broadly meaningful results. We show how complications that arise with validating using spheres can be representative of the issues that occur when modeling more complex objects. However, using spheres makes it easier to identify and understand these issues and discrepancies. We also describe how spheres present demanding problems for the CEM validation and benchmarking of both small- and large-size problems.

INTRODUCTION

Validating CEM tools can be exceedingly challenging but is necessary to develop confidence in codes before incorporating their use in any number of potential design or analysis workflows. Ideally, a fully validated tool will provide results that reflect the accuracy of the inputs and that can be trusted by users and stakeholders for decision making.

As with any scientific software, even with extensive unit and integration tests of code components (e.g., geometry processing, integrals, singularity handling, linear algebra routines, etc.), there is still a need for end-to-end runs that generate predictions to validate code accuracy [1], [2]. Many of the difficulties associated with validation arise from the dearth of quality publicly available reference data by which to assess end-to-end code accuracy.

An obvious and common choice for reference data for CEM validation is measurement data, such as anechoic chamber measurements of radar cross-section (RCS) or antenna gain [3]. However, there are significant costs associated with the collection of high-quality measurement data, including everything from building the actual validation models to costs associated with range time. In our experience, this leads to a limited number of measurements collected and even fewer repeated measurements to enable a statistical understanding of the experimental uncertainty of measurements.

Typically, then, the approach is to provide ad hoc assessments of measurement uncertainty (e.g., ± 1 dBsm) or to use the noise floor or range sensitivity as a single metric. However, this approach ignores the impact of a multitude of other sources of uncertainty in the measurements. For example, discrepancies between “as designed” and “as built” test fixtures can lead to differences in results that might be falsely attributed to code errors while actually reflecting an error in the model inputs. Additionally, even with the most careful alignment, there is likely some discrepancy between the measured and simulated angle cuts. Chamber and target mounting effects can have unexpected impacts on measurements, and so on. Absent sufficient measurement data to reach statistical significance, the complex accumulation of all sources of uncertainty must be accounted for to get a true handle on the overall experimental uncertainty associated with a reference dataset.

All of this taken together means that perceived discrepancies between reference data and CEM predictions may not, in fact, be indicative of a failed tool validation. There is significant value, then, in reference cases that have extremely low uncertainty, especially if they are sufficiently complex so as to capture many of the challenges that might arise with real-world use cases. A natural choice for scattering problems is spheres, which will be the focus of the rest of this article. Spheres have a dynamic frequency response over a wide range of frequencies and closed-form solutions for perfect electric conductors (PECs) [4], impedance boundary conditions [5], [6], dielectrics [7], and multilayer combinations of all [8]. Leveraging spherical symmetry enables the statistical evaluation of CEM predictions, including the analysis of highly structured bistatic scattering patterns.

That said, IEEE Standard 1597.1 notes some limitations in the use of spheres for validation [9], and previous versions only provided monostatic Mie series reference data for a PEC sphere

Perceived discrepancies between reference data and CEM predictions may not, in fact, be indicative of a failed tool validation.

over a small range of sizes [10]. The standard notes that spheres “may not represent the real-world problem of interest to the user.” However, given the diversity of potential inputs into a CEM tool, no matter how complex the reference problem, validated results for one model likewise do not “guarantee that simulations of reflections from [another] complex object... will produce a correct result,” so in our view, spheres are no worse than any

other choice of model. The standard does recognize that closed-form equations can be useful in understanding “the accuracy of the final results,” and we address this in greater detail.

In this article, then, we aim to illustrate some examples of how validating against spheres actually provides a range of challenges and broadly meaningful results for CEM validation. We focus on far-field scattering effects, but this general approach would be applicable to other quantities of interest, such as current, gain, near field etc. Additionally, for the purposes of conciseness and clarity, the examples we highlight in this article are PEC spheres. However, the methodologies, nuances, and recommendations discussed here apply equally well to the variety of sphere problems that can be constructed, and we strongly recommend that sphere cases be utilized in the validation of CEM codes that handle materials.

We will show how complications that arise when validating with spheres can be representative of many issues that arise when modeling more complex objects, such as mesh and model convergence. Moreover, it is easier to identify and understand discrepancies when the reference data are of exceptionally high quality. Thus, using spheres can help CEM code developers and users quantify errors and make decisions specific to their use cases if that level of error is acceptable. Spheres also present demanding problems in their own right, especially when considering the difficulties that come with CEM modeling at either extreme of the size spectrum.

All numerical simulation results presented in this article are solved using Riverside Research production- and research-grade method of moments CEM codes. Mie series results are computed using an arbitrary precision Mathematica implementation.

VALIDATION STATISTICS

In addition to the uncertainty associated with validation data, there are a number of sources of uncertainty associated with simulated results. Quantifying this uncertainty for a complex problem is not straightforward, although there is some recent work to develop methods to assist with this [11], [12], [13]. Nevertheless, one can use results from highly symmetric cases to build statistics for a CEM code’s performance.

For example, consider a nominally 1-m-radius PEC sphere at 300 MHz meshed at different densities with respect to wavelength, λ (Figure 1). Depending on the mesh density, the sphere may look more like a disco ball than a sphere,

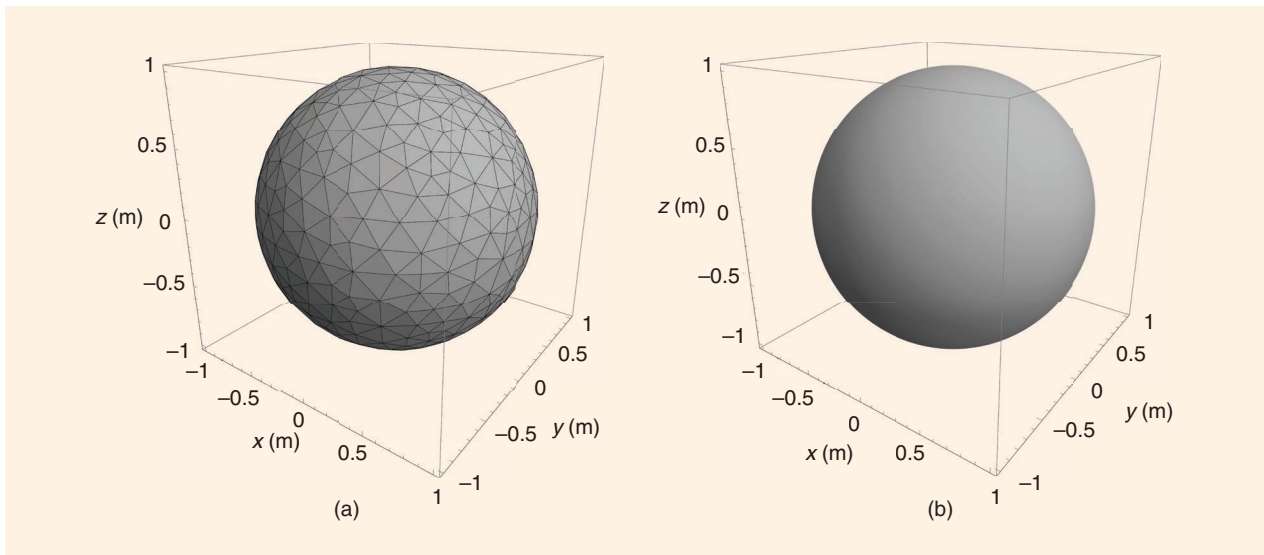


FIGURE 1. (a) Very coarse and (b) very fine meshes for a 1-m-radius PEC sphere. (a) Sphere coarsely meshed at $\lambda/6$. (b) Sphere finely meshed at $\lambda/111$.

but even at the finest meshes, we still generally expect that the discretization will lack the symmetry and smoothness of the original sphere. Thus, there will be some variability in the resulting numerical solution arising from the discretization. We now show how one can use this variation in monostatic RCS as a function of all angles for this simple and highly symmetric case to help estimate the expected uncertainty in more complex models.

Figure 2 shows the angle-dependent variation from the median monostatic RCS value for the two meshes shown in Figure 1, paying careful notice to the scale of the vertical axis. Both meshes give results that vary as a function of angle; however, the coarsely meshed sphere has variability in the first decimal place of RCS values (in dBsm), while the fine mesh has that variability in the third decimal. Many-angle RCS statistics for a range of mesh densities are provided in Figure 3, which highlights a clear relationship between mesh density and solution uncertainty; finer meshes have significantly lower variation in results compared to the coarser “disco balls.”

While we present only limited statistics here, for robust CEM validation, we recommend using more extensive analyses, including bistatics, many-angle cuts, and additional mesh densities.

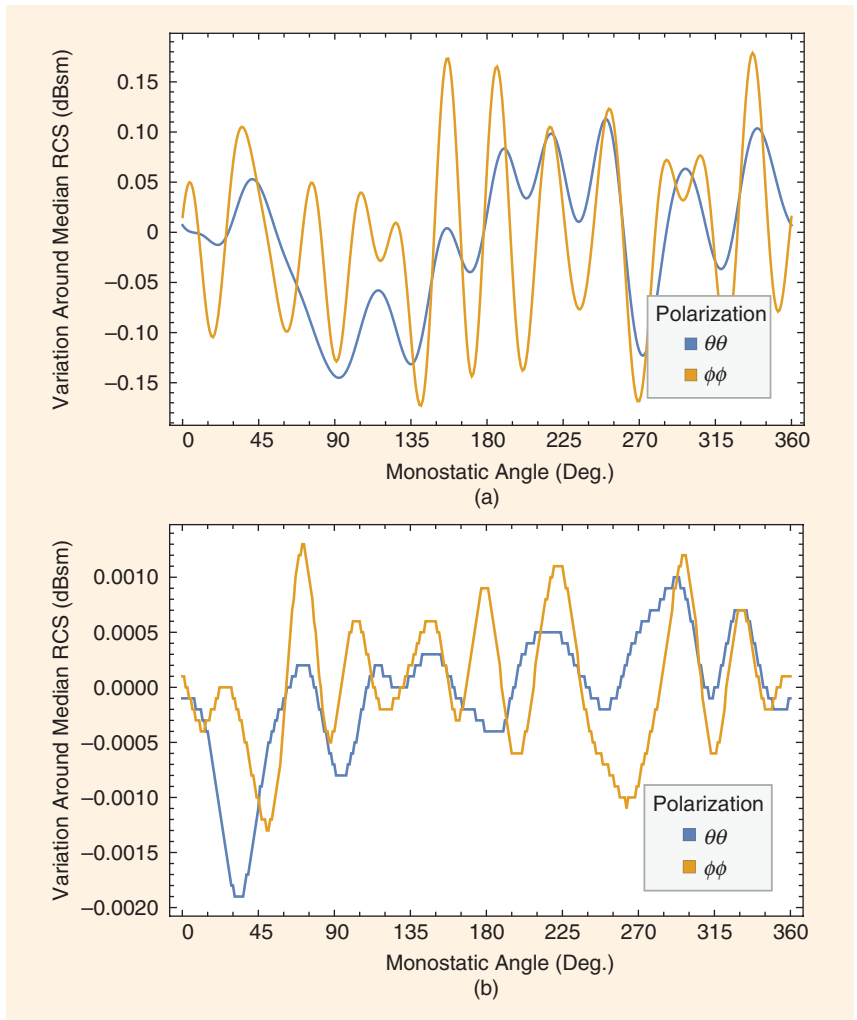


FIGURE 2. Variation in monostatic RCS cut for (a) coarse and (b) fine meshes for a 1-m-radius PEC sphere. Note the difference in scale of the vertical axes. (a) Sphere coarsely meshed at $\lambda/6$. (b) Sphere finely meshed at $\lambda/111$. Deg.: degrees.

This approach helps inform bounds on comparisons to reference data in validation, and these uncertainties should be accounted for when validating a CEM code or performing any other analysis. Thus, in the remainder of this article, we include error bars on results leveraging this approach whenever possible.

Furthermore, validating a CEM code using spheres in this manner enables a CEM developer to provide their users with standard guidelines for expected uncertainty in RCS results for more complex models. This will help users and their stakeholders understand the limitations and confidence in CEM-based analyses. More generally, we also recommend following this approach and using whatever model symmetries are available in actual models of interest to evaluate the quality of CEM predictions. With a well-validated code, this can help isolate and distinguish between angle-dependent mesh-driven issues and potential underlying issues with a CEM code.

MESH AND MODEL CONVERGENCE

Many complex models that represent real-world scattering problems have curved surfaces over at least some portion of their geometry. While higher-order meshes can assist with capturing curved geometries [14], flat geometry elements are a common

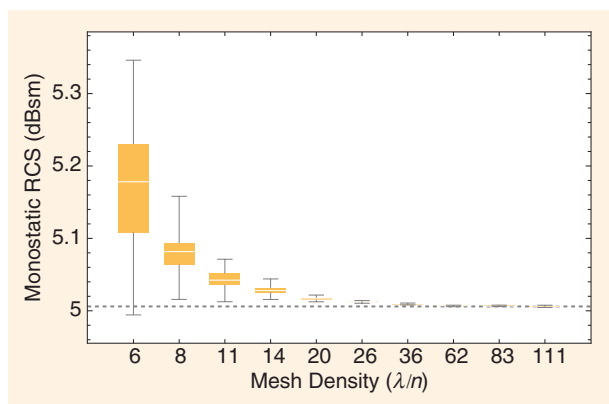


FIGURE 3. Variability in monostatic RCS statistics for a nominally 1-m PEC sphere at 300 MHz for meshes of different densities.

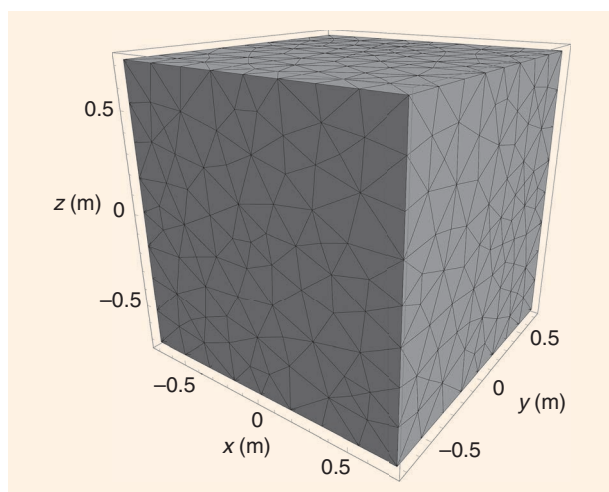


FIGURE 4. The coarse mesh of a PEC cube with $4\pi m^2$ area.

choice for discretization [15]. In these cases, it is easy to accidentally conflate mesh convergence with model convergence. Since spheres are smoothly curved everywhere, they provide a useful model by which to highlight this.

As an illustration, consider the rate of convergence of RCS with respect to mesh density for a PEC cube (Figure 4) and a sphere of the same surface area (Figure 5). In this case, we compare the sphere results to Mie theory [4], while lacking a theoretical reference, the cube results are compared to the results for the finest mesh. These results indicate that for a given mesh density, the cube appears to be more converged than the sphere. Conversely, to achieve a given percent error, the sphere requires a significantly finer mesh than the cube. This would seemingly indicate that at a specific mesh density, the CEM tool is less accurate for curved surfaces than flat surfaces. However, there is a nuance with the sphere results that, once accounted for, indicates equivalent accuracy for both flat and curved surfaces.

Consider a 2D cross-section of a meshed sphere (Figure 6), very coarsely meshed for illustrative purposes. In all the

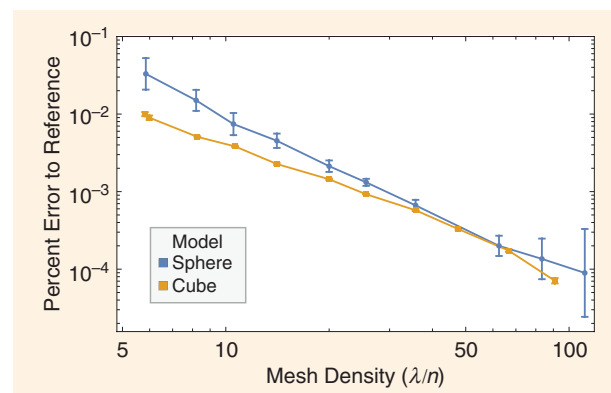


FIGURE 5. The convergence of the RCS solution with respect to mesh density for a PEC sphere and cube with $4\pi m^2$ area.

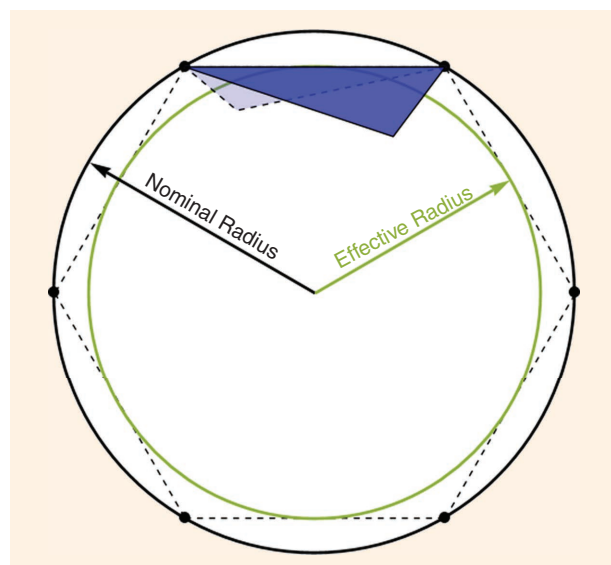


FIGURE 6. An illustration of the distinction between nominal radius (black) and effective radius (green) for a discretized curved geometry.

meshing tools we have encountered, the mesher attaches nodes to the specified curved surface (black points in the image). Then, linear mesh elements (e.g., the pair of blue triangles) cut chords *inside* the nominal specified surface (dashed lines). The resulting outcome is that the meshed surface has an effective radius (green) that is actually slightly smaller than the nominal geometry.

For a reasonably meshed surface, the difference between nominal and effective radii, δr , tends to be a small number (see Figure 7). However, depending on the scattering regime, this small discrepancy can lead to measurable differences in the expected RCS. Using Mie series results for the RCS, $\sigma = M(r)$, we can differentiate to find the relative sensitivity to small variations in radius and estimate

$$\mathcal{E} \equiv \frac{\Delta\sigma}{\sigma_0} \approx \frac{1}{\sigma_0} \frac{dM}{dr} \delta r \quad (1)$$

where σ_0 is the RCS at the radius of interest. This error varies as a function of frequency, sometimes overpredicting and sometimes underpredicting the RCS, with \mathcal{E} decreasing as ka increases (see Figure 8), where k is the wavenumber and a is the radius. Even for large spheres, this error can be quite significant, and while a smaller δr will reduce the overall error, there are other considerations when using finer meshes, as we will discuss in the “Spheres as a Challenge Problem” section.

Thus, the small discrepancies between the “as modeled” and “as specified” radii can lead to small but nonnegligible differences between theory and predictions. While we are only describing spheres here, this nuance applies to any curved shape and can confuse the interpretation of validation and mesh convergence results. If the scattered fields are indeed a sensitive function of the radius, it is still possible to get a false indication of a “nonvalidated” code or incorrect RCS predictions of an

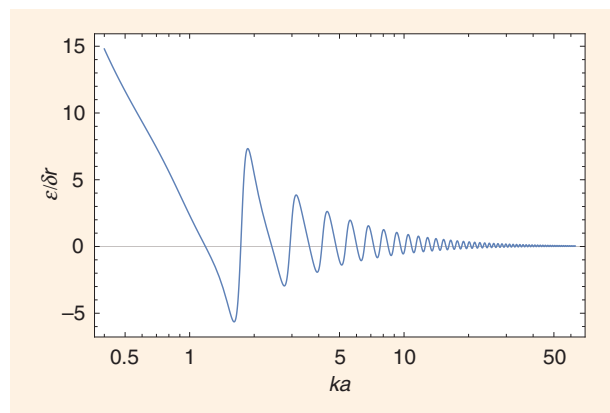


FIGURE 8. The relative theoretical error in RCS for small changes in radius.

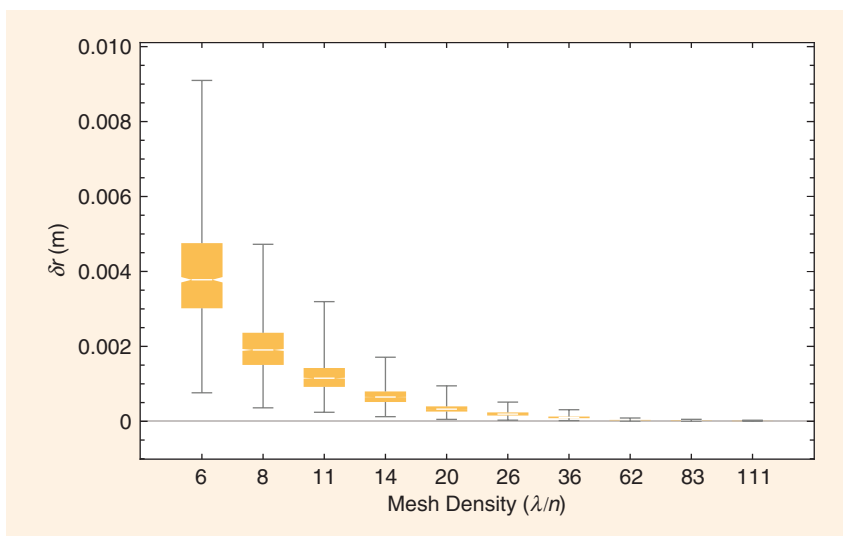


FIGURE 7. The distribution of δr for a 1-m sphere meshed to different mesh densities.

object of interest, even for a mesh density that yields converged results for other models. This is not an issue of mesh convergence as is typically understood to mean convergence to a level that captures all relevant physics. Instead, it is an issue of the convergence of the specified mesh model radius to the nominal model radius, even if the physics is fully captured.

To illustrate this, in Figure 9, we analyze the RCS results for a 1-m nominal radius PEC sphere as a function of different mesh densities. In this case, the percent error is relative to the Mie series RCS for the nominal PEC sphere. Simulated results for a meshed sphere are shown in the orange dashed curve, showing monotonic convergence to the nominal result. We also computed the Mie series RCS for a sphere with the effective radius extracted from the mesh used for each simulation, shown in blue. The uncertainty for these results is computed from variability in the RCS arising from the distribution of radii. The results for the simulated meshed model and the theoretical RCS for the effective radius case are the same (within uncertainty).

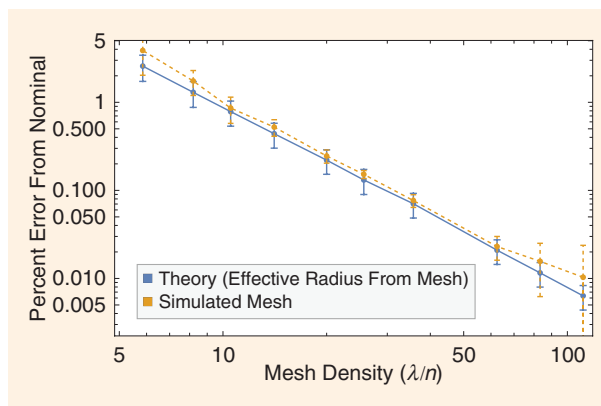


FIGURE 9. The percent error between the nominal RCS of a PEC sphere and (blue) the theoretical RCS of a sphere with an effective radius given by the meshed model or (orange, dashed) simulated results from the meshed model.

This indicates that we are able to isolate mesh convergence with respect to physics from mesh convergence with respect to the nominal model. That is, once we account for the *actual* effective mesh radius, RCS convergence in this case is largely driven by the convergence of the mesh to the nominal radius and *not* a physics-based limitation of the mesh or CEM formulation. This is further highlighted in Figure 10, which shows how the percent error computed with respect to the nominal radius is generally more than an order of magnitude greater than the error with respect to the effective meshed radius.

This insight provides guidance for code validation and CEM code execution in general. Specifically, in addition to all the concerns about “as designed” versus “as built” models, analysts must also take care to consider “as specified” versus “as meshed.” In some cases, this might require designing models for simulation with different nominal dimensions than the actual physical hardware. Note that determining how to change the nominal specification so that the resulting mesh meets the desired dimensions will usually differ based on the model, mesher, and mesh density and will likely require some experimentation to determine best practices for each application. We

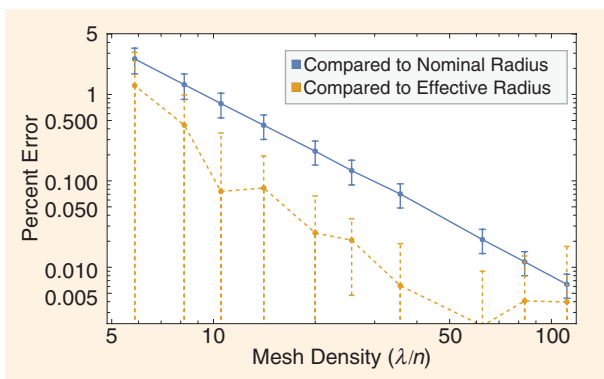


FIGURE 10. The percent error between the simulated results from meshed models and theoretical results for the nominal radius (blue) and the effective radius extracted from the meshed models (orange, dashed).

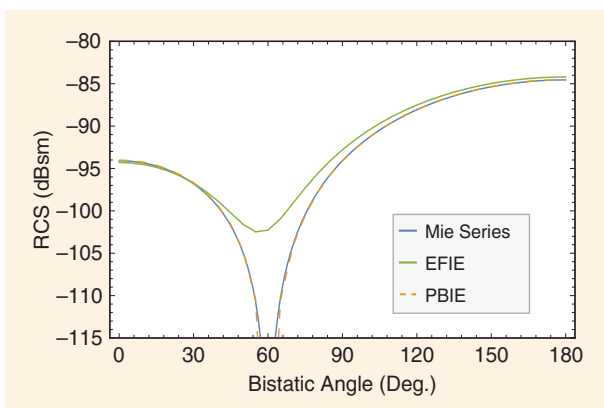


FIGURE 11. Bistatic $\theta\theta$ polarization RCS of a 1-m-radius PEC sphere solved at $\lambda = 1,000$ m. A standard electric field integral equation (EFIE) misses the null at 60° , while an implementation of [21] more accurately captures the response. PBIE: potential-based integral equation.

want to reemphasize that this experimentation is purely on the CAD/meshing side to ensure that the mesh best represents the desired geometry and is different from mesh convergence to ensure that the physics is correctly captured.

The idea that an electromagnetic model should have different properties from the mechanical model it is based on should not be a foreign one to CEM practitioners. This is, in some respects, similar to approaches to modeling wires as flat strips [16], [17], [18], where dimensions are chosen to capture the electromagnetic properties even though the model does not exactly match the mechanical dimensions. Likewise, in this case, the goal is to ensure that the mesh accurately matches the mechanical dimensions by changing the nominal model from the actual mechanical model.

SPHERES AS A CHALLENGE PROBLEM

In addition to serving as a simple representative for more complex geometries, spheres can also serve as a challenge problem for CEM methods in their own right. First, as previously discussed, meshing a nominal sphere to describe the geometry can drive the mesh density to extremely small elements. In addition to increasing the size of the resulting matrix problems that must be solved, this presents other different challenges for lower or higher frequencies.

At lower frequencies, the mesh required to describe the geometry will lead to inaccurate solutions for some standard CEM methods [15], [19], [20], which can require novel methods to accurately capture the effects. For example, Figure 11 shows how a standard electric field integral equation (EFIE) generates solutions that miss the null, while other methods capture it. Figure 12 highlights how a standard EFIE and a potential-based integral equation (PBIE) [21] demonstrate growth in the solution matrix condition number at different rates for smaller spheres (i.e., $ka < 0.1$), while other methods, like the nonresonant current-charge integral equation (NRCCIE), are more stable [22].

At higher frequencies, the problem sizes grow and require other methods to solve efficiently [23], [24], [25]. For example, using an \mathcal{H} -matrix approach, spheres tend to have a much

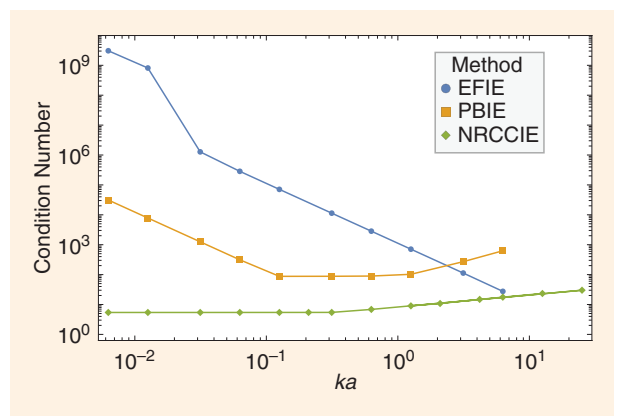


FIGURE 12. The solution matrix condition number as a function of sphere size for several methods of moments CEM methods. NRCCIE: nonresonant current-charge integral equation.

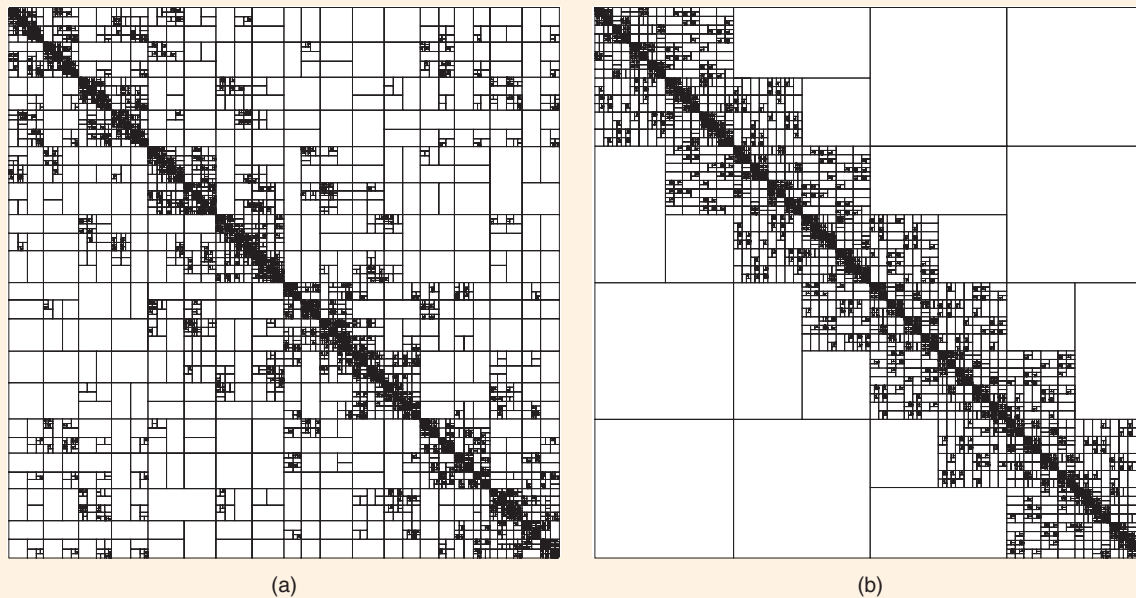


FIGURE 13. The hierarchical \mathcal{H} -matrix structure for a similarly sized (a) sphere and (b) pipe geometry, each with approximately 20 million unknowns. (a) Hierarchical matrix structure for a sphere. (b) Hierarchical matrix structure for a pipe.

more complex hierarchy and lower compression than similarly sized problems with higher aspect ratios. This is largely due to the fact that points on a sphere all have similar distances from all other points, reducing admissibility. For example, consider similarly sized spherical and pipe geometries, chosen to yield the same surface area and the same number of unknowns. That is, we choose a pipe with $\beta \equiv \text{length}/\text{radius} = 10$ and infinitely thin walls, such that $r_{\text{sphere}}^2/r_{\text{pipe}}^2 = \beta/2$. Figure 13 shows the \mathcal{H} -matrix structures resulting from problems with 20 million unknowns generated from these geometries.

In this case, the spherical geometry has a very fine structure in the hierarchy, in contrast to the pipe geometry, which has very large off-diagonal compressed blocks. We have found that the flatter hierarchy of the sphere greatly affects the performance of the resulting operations (e.g., matrix factorization and solve) since it leads to many more smaller hierarchical blocks that must be looped over and operated on. That is, solver performance suffers as entire \mathcal{H} -matrix substructures must be perused and updated for a structure that largely resembles a block low-rank matrix instead of a hierarchical matrix. In contrast, operating on the very hierarchical large off-diagonal blocks, as seen with the pipe, yields significantly less overall computational expense. We have seen indications that this trend continues with \mathcal{H}^2 -methods, with poorer scaling for both storage requirements and runtime when comparing spheres to other shapes [26]. Thus, benchmarking CEM methods using large spheres serves as a challenge case for many advanced solver methods used for higher frequency problems.

There is also a challenge in generating theoretical reference data for larger spheres. The larger the sphere, the more terms in the Mie series are required, with the larger arguments in the spherical Bessel and Hankel functions challenging many

numerical Mie series implementations. We recommend the use of arbitrary precision Mie series calculations to generate the reference data for larger spheres as the usual methods may lead to incorrect conclusions about CEM code validation (see Figure 14). For example, we found that 413 digits of precision were required when generating validation reference data for a $ka = 350$ PEC sphere. Note that although the RCS magnitude approaches πa^2 for large radii, Mie series results are still valuable for evaluating the phase as well as the near fields for larger spheres.

CONCLUSION

In this article, we illustrated some examples of how spheres provide a range of challenges and broadly meaningful results for CEM validation. We showed how the difficulties that arise when validating with spheres can be representative of many issues that occur when modeling more complex objects but can make it easier to identify and understand discrepancies.

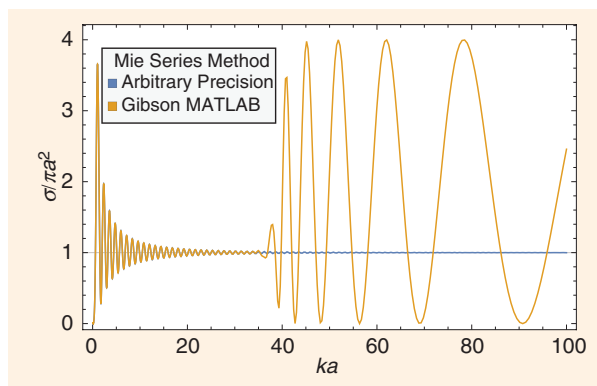


FIGURE 14. The Mie series solution for scattering cross-section computed using arbitrary precision methods and [27].

Although spheres do not typically represent interesting real-world problems in their own right, the fact that spheres have closed-form solutions and a high degree of symmetry provides high-quality reference data. Lessons learned performing CEM validation using spheres can provide developers and practitioners with useful and important results that can be more broadly applied to more “interesting” objects.

We highlighted how using spheres enables CEM developers to build meaningful statistics about code accuracy and performance, which can then be used to help interpret results from more complex models. We also illustrated how validation using spheres highlights the challenges associated with model and mesh convergence as well as the importance of distinguishing between as specified and as meshed, in addition to distinctions between as built and specified. We also showed how spheres present demanding problems for CEM validation and benchmarking, for both small and large spheres.

ACKNOWLEDGMENT

We thank our colleagues, Dr. Nathan Parzuchowski, Nathan Smith, and Marianne Spurrier, for their insightful conversations and suggestions while preparing this article. We are also appreciative of the generous Riverside Research Independent Research and Development (IRAD) funding that enabled this work. Thank you to the anonymous reviewers for their very helpful feedback as well.

AUTHOR INFORMATION

Eli Lansey (elansey@riversideresearch.org) is with Riverside Research New York, New York, NY 10038-5325 USA. He is a Member of IEEE.

Genevieve Hankins (ghankins@riversideresearch.org) is with Riverside Research New York, New York, NY 10038-5325 USA. She is a Member of IEEE.

Isroel Mandel (isroel.mandel@gmail.com) was with Riverside Research New York, New York, NY 10038-5325 USA. He is now an independent CEM consultant.

Richard Martelly (rmartelly@riversideresearch.org) is with Riverside Research New York, New York, NY 10038-5325 USA. He is a Member of IEEE.

Jocelyn Slater (j Slater@riversideresearch.org) is with Riverside Research New York, New York, NY 10038-5325 USA.

Naomi R. Greenberg (ngreenberg@riversideresearch.org) is with Riverside Research New York, New York, NY 10038-5325 USA.

REFERENCES

- [1] L. Bernstein and C. M. Yuhas, *Trustworthy Systems Through Quantitative Software Engineering*, (Quantitative Software Engineering Series). Nashville, TN, USA: Wiley, Nov. 2005.
- [2] S. Desikan and G. Ramesh, *Software Testing*. Delhi, India: Pearson Education, Jan. 2005.
- [3] UTAustinCEMGroup. “AustinCEMBenchmarks.” GitHub. [Online]. Available: <https://github.com/UTAustinCEMGroup/AustinCEMBenchmarks>, 2024
- [4] C. A. Balanis, *Advanced Engineering Electromagnetics*. New York, NY, USA: Wiley, 1989.

- [5] J. R. Wait and C. M. Jackson, “Calculations of the bistatic scattering cross section of a sphere with an impedance boundary condition,” *J. Res. Nat. Bur. Stand. Sect. D: Radio Sci.*, vol. 69D, no. 2, pp. 299–315, 1965, doi: 10.6028/jres.069D.041.
- [6] A. W. Glisson, M. Orman, F. Falco, and D. Koppel, “Electromagnetic scattering by a body of revolution with a general anisotropic impedance boundary condition,” in *Proc. IEEE Antennas Propag. Soc. Int. Symp. Dig.*, 1992, pp. 1997–2000, doi: 10.1109/APS.1992.221477.
- [7] H. J. Eom, *Electromagnetic Wave Theory for Boundary-Value Problems: An Advanced Course on Analytical Methods*. Heidelberg, Germany: Springer-Verlag, 2004.
- [8] A. A. Kishk, “Scattering from surface impedance sphere coated with dielectric materials,” in *Proc. Symp. Antenna Technol. Appl. Electromagn.*, 1988, pp. 1–6.
- [9] *IEEE Standard for Validation of Computational Electromagnetics Computer Modeling and Simulations*, IEEE Standard 1597.1-2022, 2022.
- [10] *IEEE Standard for Validation of Computational Electromagnetics Computer Modeling and Simulations*, IEEE Standard 1597.2-2010, 2010.
- [11] J. J. Harmon, C. Key, D. Estep, T. Butler, and B. M. Notaros, “Adjoint sensitivity analysis for uncertain material parameters in frequency-domain 3-D FEM,” *IEEE Trans. Antennas Propag.*, vol. 69, no. 10, pp. 6669–6679, Oct. 2021, doi: 10.1109/TAP.2021.3070059.
- [12] J. J. Harmon and B. M. Notaros, “Accelerated adaptive error control and refinement for SIE scattering problems,” *IEEE Trans. Antennas Propag.*, vol. 70, no. 10, pp. 9497–9510, Oct. 2022, doi: 10.1109/TAP.2022.3177424.
- [13] S. Kasdorf, J. J. Harmon, and B. M. Notaros, “Kriging methodology for uncertainty quantification in computational electromagnetics,” *IEEE Open J. Antennas Propag.*, vol. 5, no. 2, pp. 474–486, Apr. 2024, doi: 10.1109/OJAP.2024.3363730.
- [14] A. F. Peterson, “Cell curvature and far-field superconvergence in numerical solutions of electromagnetic integral equations,” *Int. J. Antennas Propag.*, vol. 2016, pp. 1–7, May 2016, doi: 10.1155/2016/9808637.
- [15] S. Rao, D. Wilton, and A. Glisson, “Electromagnetic scattering by surfaces of arbitrary shape,” *IEEE Trans. Antennas Propag.*, vol. 30, no. 3, pp. 409–418, May 1982, doi: 10.1109/TAP.1982.1142818.
- [16] C. Butler, “The equivalent radius of a narrow conducting strip,” *IEEE Trans. Antennas Propag.*, vol. 30, no. 4, pp. 755–758, Jul. 1982, doi: 10.1109/TAP.1982.1142839.
- [17] C. A. Balanis, *Antenna Theory*, 4th ed. Hoboken, NJ, USA: Wiley, Jan. 2016.
- [18] J. Volakis, *Antenna Engineering Handbook*, 5th ed. Columbus, OH, USA: McGraw-Hill, Jan. 2019.
- [19] L. N. Medgyesi-Mitschang, J. M. Putnam, and M. B. Gedera, “Generalized method of moments for three-dimensional penetrable scatterers,” *J. Opt. Soc. Am. A*, vol. 11, no. 4, Apr. 1994, Art. no. 1383, doi: 10.1364/JOSAA.11.001383.
- [20] W. C. Chew, M. S. Tong, and B. Hu, *Integral Equation Methods for Electromagnetic and Elastic Waves* (Synthesis Lectures on Computational Electromagnetics). Cham, Switzerland: Springer-Verlag, 2009.
- [21] Q. S. Liu, S. Sun, and W. C. Chew, “A potential-based integral equation method for low-frequency electromagnetic problems,” *IEEE Trans. Antennas Propag.*, vol. 66, no. 3, pp. 1413–1426, Mar. 2018, doi: 10.1109/TAP.2018.2794388.
- [22] M. Taskinen and P. Yla-Oijala, “Current and charge integral equation formulation,” *IEEE Trans. Antennas Propag.*, vol. 54, no. 1, pp. 58–67, Jan. 2006, doi: 10.1109/TAP.2005.861580.
- [23] M. Bebendorf, *Hierarchical Matrices: A Means to Efficiently Solve Elliptic Boundary Value Problems* (Lecture notes in Computational Science and Engineering). Berlin, Germany: Springer-Verlag, 2008.
- [24] Z. Jiang, Y. Sheng and S. Shen, “Multilevel fast multipole algorithm-based direct solution for analysis of electromagnetic problems,” *IEEE Trans. Antennas Propag.*, vol. 59, no. 9, pp. 3491–3494, Sep. 2011, doi: 10.1109/TAP.2011.2161560.
- [25] W. Hackbusch, *Hierarchical Matrices: Algorithms and Analysis* (Springer Series in Computational Mathematics), vol. 49. Berlin, Germany: Springer-Verlag.
- [26] N. M. Parzuchowski, B. Hall, I. M. Mandel, I. Holloway, and E. Lansey, “A recompressed nested cross approximation for electrically large bodies,” *IEEE Trans. Antennas Propag.*, vol. 71, no. 3, pp. 2587–2595, Mar. 2023, doi: 10.1109/TAP.2023.3237277.
- [27] W. Gibson. “Scattered Field of a Conducting and Stratified Spheres, v1.5.0.0.” MathWorks. [Online]. Available: <https://www.mathworks.com/matlabcentral/fileexchange/20430-scattered-field-of-a-conducting-and-stratified-spheres>

